Dalton Transactions

PAPER

View Article Online
View Journal | View Issue

Cite this: *Dalton Trans.*, 2017, **46**, 1455

Cu(I) and Ag(I) complex formation with the hydrophilic phosphine 1,3,5-triaza-7-phosphadamantane in different ionic media. How to estimate the effect of a complexing medium†

Francesco Endrizzi,*[a,b] Plinio Di Bernardo,[a] Pier Luigi Zanonato,[a] Francesco Tisato,[c] Marina Porchia,[c] Abdirisak Ahmed Isse,[a] Andrea Melchior[d] and Marilena Tolazzi[d]

The complexes of Cu(I) and Ag(I) with 1,3,5-triaza-7-phosphadamantane (PTA) are currently studied for their potential clinical use as anticancer agents, given the cytotoxicity they exhibited *in vitro* towards a panel of several human tumor cell lines. These metallodrugs are prepared in the form of $[M(PTA)_4]^+$ ($M = Cu^+$, Ag^+) compounds and dissolved in physiological solution for their administration. However, the nature of the species involved in the cytotoxic activity of the compounds is often unknown. In the present work, the thermodynamics of formation of the complexes of Cu(I) and Ag(I) with PTA in aqueous solution is investigated by means of potentiometric, spectrophotometric and microcalorimetric methods. The results show that both metal(I) ions form up to four successive complexes with PTA. The formation of Ag(I) complexes is studied at 298.15 K in 0.1 M $NaNO_3$ whereas the formation of the Cu(I) one is studied in 1 M NaCl, where Cu(I) is stabilized by the formation of three successive chloro-complexes. Therefore, for this latter system, conditional stability constants and thermodynamic data are obtained. To estimate the affinity of Cu(I) for PTA in the absence of chloride, Density Functional Theory (DFT) calculations have been done to obtain the stoichiometry and the relative stability of the possible Cu/PTA/Cl species. Results indicate that one chloride ion is involved in the formation of the first two complexes of Cu(I) ([CuCl(PTA)] and $[CuCl(PTA)_2]$) whereas it is absent in the successive ones ($[Cu(PTA)_3]^+$ and $[Cu(PTA)_4]^+$). The combination of DFT results and thermodynamic experimental data has been used to estimate the stability constants of the four $[Cu(PTA)_n]^+$ ($n = 1–4$) complexes in an ideal non-complexing medium. The calculated stability constants are higher than the corresponding conditional values and show that PTA prefers Cu(I) to the Ag(I) ion. The approach used here to estimate the hidden role of chloride on the conditional stability constants of Cu(I) complexes may be applied to any Cu(I)/ligand system, provided that the stoichiometry of the species in NaCl solution is known. The speciation for the two systems shows that the $[M(PTA)_4]^+$ ($M = Cu^+$, Ag^+) complexes present in the metallodrugs are dissociated into lower stoichiometry species when diluted to the micromolar concentration range, typical of the *in vitro* biological testing. Accordingly, $[Cu(PTA)_2]^+$, $[Cu(PTA)_3]^+$ and $[Ag(PTA)_2]^+$ are predicted to be the species actually involved in the cytotoxic activity of these compounds.

Received 4th November 2016,
Accepted 21st December 2016

DOI: 10.1039/c6dt04221j

rsc.li/dalton

Introduction

The interest in copper-based metallodrugs is due to the fact that copper, unlike platinum which is often employed in cancer chemotherapy, is an ubiquitous bioelement involved in several processes of metabolic enzymes in living organisms.[1] In addition, altered levels of intracellular copper are related to both some genetic disorders and other serious pathologies such as prostate and lung cancer.[2] On the basis of these pieces of evidence, several therapies based on the administration of copper salts in the presence of chelating agents capable of transporting this bioelement have recently been developed.[2]

[a]*Dipartimento di Scienze Chimiche, Università di Padova, Via Marzolo 1, 35131 Padova, Italy. E-mail: francesco.endrizzi@kit.edu*
[b]*Institute for Nuclear Waste Disposal, Karlsruhe Institute of Technology, Hermann-von-Helmholtz-Platz 1, 76344 Eggenstein-Leopoldshafen, Germany*
[c]*CNR – ICMATE, Corso Stati Uniti 4, 35127 Padova, Italy*
[d]*Dipartimento Politecnico di Ingegneria e Architettura, Università di Udine, Laboratori di Scienze e Tecnologie Chimiche, via Cotonificio 108, 33100 Udine, Italy*
†Electronic supplementary information (ESI) available. See DOI: 10.1039/c6dt04221j

Intracellular copper intake in the human body is strictly regulated by a complex membrane protein system (hCTR1) with an active transport function.[3–5] These proteins contain histidine-rich and methionine-rich amino acidic sequences, which are putative binding sites for Cu(I).[6,7] In fact, several studies, based on *in vitro* and competition experiments between these substrates and monovalent Cu(I) and Ag(I) and divalent Cu(II) and Zn(II), demonstrated that these sites show a specific affinity for Cu(I) rather than for the Cu(II) ion.[6,8–10] Despite these pieces of evidence, most of the research on copper compounds with potential anti-tumor activity mainly focused on Cu(II) derivatives[2] and only little attention has been paid to Cu(I) compounds.[11] A new class of Cu(I) compounds with hydrophilic phosphines (Scheme 1), characterized by both high thermodynamic stability and good solubility in aqueous solution, has recently been proposed.[12–14] Among these compounds, species including mono-dentate phosphine exhibit good to moderate cytotoxic activity *in vitro*, whereas the activity of complexes comprising chelate phosphines is negligible.[13] The cytotoxic activity of these Cu(I)-based metallodrugs is considered to be linked to the complex abilities of binding biological substrates after dissociation of one or more phosphines. In agreement with this suggestion, ESI-MS experiments showed that the chelate complex (**1**) retains its tetracoordination at the high dilutions required by *in vitro* and MS experiments (10^{-5}–10^{-6} mol L^{-1}), while the complexes containing mono-dentate phosphines, (**2**) and (**3**), are partially dissociated.[12,15] Therefore, the nature and stability of the species of these Cu(I)-based compounds seems to be of fundamental importance for their biological activity.

In this work, solution equilibria for the formation of Cu(I) and Ag(I) complexes with the phosphine 1,3,5 triaza-7-phosphadamantane (PTA, Scheme 1) are reported. While coordination compounds of Cu(I) and Ag(I) with PTA are known and well-characterized in the solid state[16–22] little is known about their speciation in concentrated chloride solutions. In the present study we used potentiometric, microcalorimetric, and spectrophotometric techniques to determine the complete set of conditional thermodynamic functions (ΔG_j°, ΔH_j°, ΔS_j°, j = 1–4) for the complexation of Cu(I) and Ag(I) with PTA. Experiments on the Cu(I)/PTA system were carried out in the complexing medium 1 M NaCl, where Cu(I) is stabilized by the formation of three successive chloro-complexes.[23] The study has been also extended to the complexation of Ag(I) by PTA since the Ag(I)/PTA complexes have also already been tested for their cytotoxicity.[11] Density Functional Theory (DFT) calculations have been employed to assess the nature and stoichiometry of the prevailing Cu(I) species in solution in the presence and absence of PTA. This computational approach has been successfully employed to obtain reliable structural and thermochemical data for metal complex formation in the gas phase and aqueous solution.[24–34] The combined results from the thermodynamic studies and DFT calculations are used to propose a relationship between the stability in solution of the $[M(PTA)_4][X]$ compounds (X = BF_4^-, PF_6^-, Fig. 1) and their cytotoxic activity.

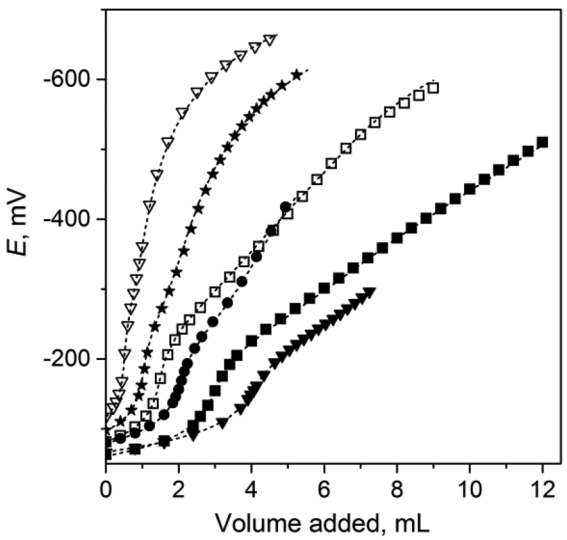

Fig. 1 Potentiometric titrations for the Ag(I)–H–PTA system: symbols: experimental values, dotted lines: calculated potentials. (■) Tit. 1, $[Ag^+]_0 = 1.8 \times 10^{-3}$ M, $[H^+]_0 = 0.99 \times 10^{-3}$ M, $[PTA]_{tit} = 0.010$ M, $[H^+]_{tit} = 1.0 \times 10^{-3}$ M; (□) Tit. 2, $[Ag^+]_0 = 0.95 \times 10^{-3}$ M, $[H^+]_0 = 1.0 \times 10^{-3}$ M, $[PTA]_{tit} = 0.010$ M, $[H^+]_{tit} = 1.0 \times 10^{-3}$ M; (★) Tit. 3, $[Ag^+]_0 = 0.49 \times 10^{-3}$ M, $[PTA]_{tit} = 0.010$ M; (●) Tit. 4, $[Ag^+]_0 = 1.0 \times 10^{-3}$ M, $[PTA]_{tit} = 0.010$ M; (▼) Tit. 5, $[Ag^+]_0 = 2.0 \times 10^{-3}$ M, $[PTA]_{tit} = 0.010$ M; (▽) Tit 6 $[Ag^+]_0 = 0.26 \times 10^{-3}$ M, $[PTA]_{tit} = 0.010$ M (analytical concentrations of the species are reported in Table S3†). Some experimental points were omitted for clarity.

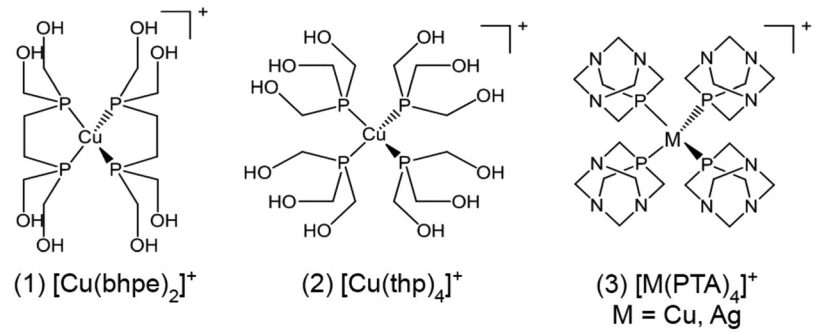

Scheme 1 The Cu(I) and Ag(I) complexes with hydrophilic phosphines recently synthesized as perspective antitumor agents.

Experimental

Chemicals

1,3,5-Triaza-7-phosphadamantane (PTA) was prepared according to ref. 35. The crude product, once dried under vacuum, was dissolved in $CHCl_3$ in order to remove NaCl, formed as a byproduct. Chloroform was then evaporated under vacuum and replaced by methanol to eliminate insoluble PTA oxidation products. Finally, PTA was recovered by solvent removal and purified by recrystallization from water at room temperature. Copper(II) chloride dihydrate (Aldrich, >99.99%), $AgNO_3$ (Aldrich, >99%) and $NaNO_3$ (Aldrich, >99.99%) were used as received. NaCl (Aldrich, 99.0%) was purified by recrystallization from milliQ water before its use. Copper(I) chloride was prepared by comproportionation of Cu(II) and metallic copper in a chloride medium. All other reagents were purified and standardized according to common analytical procedures.[36,37]

Stock solutions of Cu(I) and Ag(I) (~0.05 M) were prepared by dissolving appropriate amounts of salts ($AgNO_3$ or CuCl) in ionic media adjusted to 0.1 M (Na/Ag)NO_3 or 1.0 M (Na/Cu)Cl, respectively. In the same way, the stock solutions of PTA (0.05 or 0.10 M) were prepared by dissolving solid PTA in 0.1 M $NaNO_3$ or 1.0 M NaCl. MilliQ-grade water used for the preparation of the stock solutions was freshly boiled and degassed under an argon stream. Solutions were prepared, handled and stored in a nitrogen glovebox, in order to avoid oxygen contamination.

Thermodynamic studies

The formation of the Ag(I)–PTA species was studied in 0.1 M $NaNO_3$ while that of the Cu(I) complexes was studied in 1.0 M NaCl, to prevent the disproportionation of Cu(I), otherwise spontaneously occurring in aqueous solution. In 1.0 M chloride medium Cu(I) is stabilized by the formation of three successive complexes with the general formula $[CuCl_m]^{1-m}$ (m = 1–3).[23,38–40] According to the stability constants of these species‡ and under anoxic conditions, $[CuCl_2]^-$ (~66%) and $[CuCl_3]^{2-}$ (~34%) are the main Cu(I) species present in solutions with 1.0 M NaCl. A better representation of the complexation equilibria of Cu(I) with PTA in 1.0 M NaCl should therefore consider the simultaneous occurrence of reactions (1) and (2) where the phosphine complexes result from a total or partial substitution of chloride in the coordination sphere of the metal ion.

$$[CuCl_2]^- + n\text{PTA} \rightleftarrows [Cu(\text{PTA})_n Cl_m]^{(1-m)} + (2-m)\ Cl^- \quad (1)$$

$$[CuCl_3]^{2-} + n\text{PTA} \rightleftarrows [Cu(\text{PTA})_n Cl_m]^{(1-m)} + (3-m)\ Cl^- \quad (2)$$

Hence, the stability constants and thermodynamic functions provided by the present experiments according to general eqn (3), must be considered conditional when M = Cu(I), whereas they reflect the true affinity of the metal ion for the phosphine in the non-complexing medium 0.1 M $NaNO_3$, when M = Ag(I).

$$M^+ + n\text{PTA} \rightleftarrows M(\text{PTA})_n{}^+;\ \beta_n = [M(\text{PTA})_n{}^+] \cdot [M^+]^{-1} \cdot [\text{PTA}]^{-n} \quad (3)$$

Experimental techniques

Cyclic voltammetry (CV). In order to gain insights into the redox properties of PTA and its Cu(I) and Cu(II) complexes, some preliminary cyclic voltammetry (CV) experiments were carried out, prior to thermodynamic studies, with a Metrohm Autolab instrument, in a thermostated cell at 298.15 ± 0.10 K. Platinum working counter electrodes and a saturated calomel electrode, SCE, as the reference, were used. CV curves were collected and processed with the GPES software provided by the manufacturer. Solutions of CuCl or $CuCl_2$ (from 1.0×10^{-3} to 0.010 M in 1.0 M NaCl) were prepared directly in the measuring cell. Increasing amounts of PTA were then added to the cell solution and CV curves were collected. In all experiments, the solution was thoroughly degassed and maintained under argon in order to avoid atmospheric oxygen contamination.

Potentiometry. Potentiometry was used to evaluate the protonation constant of PTA and the complexation reactions in the Ag(I)–PTA system. In both cases, the electrode potential (E, mV) was measured with an Amel 2335 digital pH meter.

A series of acid–base volumetric titrations were carried out in the appropriate ionic medium (1 M NaCl or 0.1 M $NaNO_3$) to study the protonation of PTA, occurring at one of its aminic functions.[22] A combined glass electrode (Metrohm Unitrode 6.0259.100) was used to monitor pH_M ($-\log[H^+]$) changes during the experiments. Prior to each titration, acid–base neutralizations with standard HCl or HNO_3 and NaOH solutions were done to calibrate the electrode chain and obtain the hydrogen ion concentration.

The formation of Ag(I)–PTA complexes was studied with a series of volumetric titrations where solutions of 0.010 M PTA were added to solutions of $AgNO_3$ (0.25×10^{-3}–1.8×10^{-3} M) in 0.1 M $NaNO_3$ at 298.15 ± 0.10 K (ESI, Table S1†). A silver electrode (Metrohm Combined Ag-ring, model 6.0350.100) was used to determine the changes of the concentration of Ag(I). The Nernstian behavior of the electrode was checked with appropriate blank titrations. Typically, experiments were designed to study the complex formation under conditions of neutral or slightly alkaline pH values, where only complexes with the neutral PTA are formed. However, some titrations were also run at pH ~ 3–5 to determine the stability constants of Ag(I) with $H(\text{PTA})^+$, a less relevant species in the context of this study.

The experimental data were processed with the least-squares minimization program Hyperquad2006.[41]

UV-Vis spectrophotometry. Spectrophotometry is widely used to study reaction equilibria.[42,43] In the present work, it was used as the first experimental technique to determine the formation constants of Cu(I)–PTA complexes in 1.0 M NaCl. A series of batch solutions of Cu(I) (50×10^{-6}–0.045 M) containing increasing molar ratios of PTA/Cu(I) (R_c = from 0 to 10) were prepared in 1.0 M NaCl. Near-neutral or slightly alkaline

‡ $\log\beta_1 = 2.68$, $\log\beta_2 = 5.07$, $\log\beta_3 = 4.78$, calculated at μ = 1.0 M NaCl, according to the Pitzer parameters in ref. 23.

conditions were used, to limit the study to the formation of the sole complexes $[Cu(PTA)_n]^+$ (eqn (1) and (2)). During the experiments, the cell temperature was maintained at 298.0 ± 0.1 K with a dedicated Peltier thermostat. Absorbance spectra of these solutions were collected with a Varian Cary 4000 spectrophotometer in the wavelength range 210–340 nm, where the characteristic charge-transfer bands for the phosphine (210–220 nm) and those for the $[Cu(PTA)_n]^+$ complexes (220–300 nm) appear. Experimental data were processed with the HypSpec 2008 program[41] (analytical data summarized in the ESI, Table S2†).

Microcalorimetry. An independent determination of the formation constants and the related reaction enthalpies of the Cu(I)–PTA complexes was obtained by microcalorimetry. A series of titrations were carried out with a TAM II (Thermometric) isothermal microcalorimeter (analytical details are given in the ESI, Table S3†). In a typical experiment, designed to obtain the thermodynamic formation parameters (ΔG and ΔH) of the first two successive Cu–PTA complexes, increasing volumes of a PTA solution (0.03–0.05 M) were added to solutions of Cu(I) (0.2×10^{-3}–0.5×10^{-3} M). Further titrations were also carried out to obtain accurate values of the formation enthalpies of the more substituted complexes $[Cu(PTA)_3]^+$ and $[Cu(PTA)_4]^+$. In this case, solutions of PTA 0.5×10^{-3} to 0.010 M in the calorimeter cell were titrated with increasing volumes of Cu(I) solutions (0.010 M). In order to minimize the risk of reagent contamination by atmospheric oxygen, the calorimeter cell, together with the syringe containing the titrant, was assembled in a N_2 glovebox. For each titration run, n experimental values of the heat produced in the calorimeter vessel ($Q_{ex,j}, j = 1, 2, ..., n$) were collected. These values were corrected for the heat of dilution of the titrant ($Q_{dil,j}$), determined in separate runs. The net reaction heats, $Q_{obs,j} = Q_{ex,j} - Q_{dil,j}$ were then used as input data for the data fitting program (LetaCalPd),[44,45] which minimizes the quantity $\sum_n (Q_{obs,j} - Q_{calc,j})^2$. The microcalorimetric titrations on the system Ag(I)–PTA/$HPTA^+$ were carried out in 0.1 $NaNO_3$ at 298.15 K according to the same procedure described above (see the ESI, Table S1† for analytical details).

DFT calculations. Density functional theory (DFT) calculations on Cu(I)–PTA complexes were carried out using the three-parameter hybrid functional B3LYP,[46,47] which was previously shown to produce reliable structural and thermochemical parameters for monovalent d^{10} complexes.[26,27,31]

The Stuttgart–Dresden effective core potential (ECP)[48] was employed for copper, while other elements were treated using a 6-311++G(2d,p) Gaussian-type basis set. Geometry optimizations, carried out in vacuum, produced minimum structures, since no imaginary frequencies were found. Reactant and product free energies in the gas phase (G°_{gas}) were computed by adding to the electronic energy the zero point energy and thermal corrections calculated using the rigid rotor and harmonic oscillator approximations. Solvation free energies (ΔG°_{solv}) have been calculated by using the polarizable continuum model (PCM)[49] for which the cavity has been constructed using the UFF radii for the spheres centered on each atom of the solute. It also has to be taken into account that the gas-phase free energies (G°_{gas}) are calculated with the standard state of an ideal gas at 1 atm, but the solvation free energies are computed for a 1 M standard state.[50] Thus, the free energy in water (G°_{water}) has to be calculated including the term correcting for the change of the standard state: $G^\circ_{water} = G^\circ_{gas} - RT\ln(V^{-1}) + \Delta G^\circ_{solv}$, where V is the molar volume of an ideal gas at a temperature T and R is the universal ideal gas constant. At 298.15 K this correction increases G°_{water} by 7.91 kJ mol^{-1}. For water an additional correction has to be applied (9.96 kJ mol^{-1}), to go from the 1 M standard state to the "pure liquid" (55.34 M) state. All calculations have been carried out with Gaussian09.[51]

Results and discussion

Thermodynamic studies

The thermodynamic data for the formation of Ag(I)– and Cu(I)–PTA complexes are shown in Table 1, together with the relative data for the protonation of PTA in the two media. In general, the formation thermodynamics of these species are driven by the negative reaction enthalpies, in agreement with the general HSAB theory for interactions involving metals and ligands with a soft character.[52]

Data from the potentiometric titrations obtained for the Ag(I)–PTA complexes are shown in Fig. 1 and representative results of microcalorimetric titrations are reported in Fig. 2. Under neutral to slightly alkaline conditions, Ag(I) forms four mononuclear successive complexes with PTA. The other three species contain the protonated phosphine form in the acidic pH region (pH < 5).

The first Ag/PTA complex is considerably stronger that the second. A comparison of the thermodynamic data for the formation of these species ($\log K_{1,Ag} \gg \log K_{2,Ag}$; $-\Delta H_{1,Ag} > -\Delta H_{2,Ag}$; $T\Delta S_{1,Ag} \approx T\Delta S_{2,Ag}$) suggests that this can be due to the particular nature of the silver aquo-ion in solution. An EXAFS study showed that the Ag(I) aquo-ion is tetra-coordinated with a distorted tetrahedral geometry.[53] In particular, it was found that Ag(I) coordinates strongly to two solvent molecules with a significant covalent contribution, leading to a linear structure and two other molecules, with a weak electrostatic interaction, which significantly alters the structure toward a distorted tetrahedron.[53] The comparison between the stepwise enthalpies for the formation of the first two complexes ($-\Delta H_{1,Ag} > -\Delta H_{2,Ag}$) suggests that the coordination of the first PTA occurs with a relatively modest energy demand, compatible with the removal of the two weakly-bound water molecules.

The stepwise reaction entropy for the formation of $[Ag(PTA)_2]^+$, $T\Delta S_{2,Ag}$, unfavorable as $T\Delta S_{1,Ag}$, also suggests that the major desolvation of the metal ion begins in the second step, involving the replacement of the more tightly bonded water molecules. Perhaps, this also partially occurs in the formation of the third complex, even if at this stage[54] the severe conformational demands might play a negative effect on the complex formation ($\log K_{2,Ag} > \log K_{3,Ag}$; $-\Delta H_{2,Ag} > -\Delta H_{3,Ag}$;

Table 1 The overall and stepwise formation constants of H(PTA), M(I)–PTA and M(I)–(HPTA) complexes and the related thermodynamic functions (M = Cu or Ag, L = PTA). Ionic medium: 1.0 M NaCl for M = Cu; 0.1 M $NaNO_3$ for M = Ag; T = 298 K. The different experimental techniques used to obtain the successive $\log \beta_j$ values are indicated in the column heads. Ionic charges are omitted

	M = Cu					M = Ag			
Overall	$\log \beta_{j,Cu} \pm 3\sigma$ Uv-Vis	$\log \beta_{j,Cu} \pm 3\sigma$ microcal.	$\Delta G_{j,Cu} \pm 3\sigma$ kJ mol^{-1}	$\Delta H_{j,Cu} \pm 3\sigma$ kJ mol^{-1}	$T\Delta S_{j,Cu} \pm 3\sigma$ kJ mol^{-1}	$\log \beta_{j,Ag} \pm 3\sigma$ potentiometry	$\Delta G_{j,Ag} \pm 3\sigma$ kJ mol^{-1}	$\Delta H_{j,Ag} \pm 3\sigma$ kJ mol^{-1}	$T\Delta S_{j,Ag} \pm 3\sigma$ kJ mol^{-1}
M + L ⇄ ML	6.36 ± 0.11	6.3 ± 0.6	−36.0 ± 3.3	−53.0 ± 1.7	−17 ± 4	8.19 ± 0.01	−46.75 ± 0.06	−56.3 ± 0.5	−9.6 ± 0.5
M + 2L ⇄ ML_2	12.0 ± 0.6	12.1 ± 0.4	−69.1 ± 2.3	−110 ± 5	−41 ± 6	13.67 ± 0.02	−78.0 ± 0.1	−97.7 ± 0.7	−19.7 ± 0.7
M + 3L ⇄ ML_3	18.2 ± 0.2	17.7 ± 0.6	−101 ± 3.4	−148 ± 1.2	−47 ± 4	17.67 ± 0.02	−100.9 ± 0.1	−135.6 ± 0.9	−34.7 ± 0.9
M + 4L ⇄ ML_4	22.5 ± 0.2	21.4 ± 0.6	−122 ± 4	−188.0 ± 0.8	−66 ± 4	20.35 ± 0.12	−116.2 ± 0.7	−177.3 ± 1.8	−61.1 ± 1.9
M + H + L ⇄ MHL	—	11.2 ± 0.8	−64 ± 5	−67.2 ± 1.2	−3 ± 4	12.02 ± 0.01	−68.62 ± 0.06	−61.6 ± 1.3	7.0 ± 1.3
M + H + 2L ⇄ MHL_2	—	—	—	—	—	17.72 ± 0.04	−101.2 ± 0.2	−105 ± 6	−4 ± 6
M + 2H + 2L ⇄ MH_2L_2	—	20.8 ± 0.7	−119 ± 4	−160 ± 4	−41 ± 6	21.14 ± 0.02	−120.7 ± 0.1	−112 ± 4	8 ± 4
M + H + 3L ⇄ MHL_3	—	22.0 ± 0.8	−126 ± 5	−170 ± 7	−44 ± 8	—	—	—	—
M + 2H + 3L ⇄ MH_2L_3	—	—	—	—	—	26.40 ± 0.09	−150.7 ± 0.5	−135 ± 8	−15 ± 8
H + L ⇄ HL	—	5.94 ± 0.25[a]	−33.9 ± 1.4	−17.8 ± 0.6	16.1 ± 1.5	5.72 ± 0.01[b]	−32.65 ± 0.06	−15.6 ± 0.3	17.1 ± 0.3
Stepwise	$\log K_{j,Cu} \pm 3\sigma$ (Uv-Vis)	$\log K_{j,Cu} \pm 3\sigma$ (microcal.)	$\Delta G_{j,Cu} \pm 3\sigma$ kJ mol^{-1}	$\Delta H_{j,Cu} \pm 3\sigma$ kJ mol^{-1}	$T\Delta S_{j,Cu} \pm 3\sigma$ kJ mol^{-1}	$\log K_{j,Ag} \pm 3\sigma$ potentiometry	$\Delta G_{j,Ag} \pm 3\sigma$ kJ mol^{-1}	$\Delta H_{j,Ag} \pm 3\sigma$ kJ mol^{-1}	$T\Delta S_{j,Ag} \pm 3\sigma$ kJ mol^{-1}
M + L ⇄ ML	6.36 ± 0.11	6.3 ± 0.6	−36.0 ± 3.3	−53.0 ± 1.7	−17 ± 4	8.19 ± 0.01	−46.75 ± 0.06	−56.3 ± 0.5	−9.6 ± 0.5
ML + L ⇄ ML_2	5.6 ± 0.6	5.8 ± 0.7	−33 ± 5	−57 ± 5	−24 ± 7	5.48 ± 0.02	−31.3 ± 0.1	−41.4 ± 0.9	−10.1 ± 0.9
ML_2 + L ⇄ ML_3	6.2 ± 0.6	5.6 ± 0.7	−32 ± 4	−38 ± 5	−6 ± 6	4.00 ± 0.03	−22.9 ± 0.1	−37.6 ± 1.1	−14.7 ± 1.1
ML_3 + L ⇄ ML_4	3.7 ± 0.2	3.7 ± 0.8	−21 ± 5	−40.0 ± 1.4	−19 ± 5	2.68 ± 0.12	−15.3 ± 2.0	−41.7 ± 2.0	−26 ± 3
M + HL ⇄ M(HL)	—	5.3 ± 0.8	−30 ± 5	−49.4 ± 1.3	−20 ± 5	6.30 ± 0.01	−35.96 ± 0.08	−46.0 ± 1.3	−10.0 ± 1.3
M(HL) + HL ⇄ $M(HL)_2$	—	3.7 ± 1.1	−21 ± 6	−75 ± 4	−53 ± 7	3.40 ± 0.02	−19.4 ± 0.1	−35 ± 5	−16 ± 5

[a] Determined with potentiometry in 1.0 M NaCl. [b] Determined with potentiometry in 0.1 M $NaNO_3$.

Fig. 2 The overall experimental heat *vs.* the titrant volume for some representative titrations: (□) Tit. 1, $[PTA]_0 = 5.1 \times 10^{-3}$ M, $[Ag^+]_{tit} = 0.10$ M; (△) Tit. 2, $[PTA]_0 = 1.0 \times 10^{-3}$ M, $[Ag^+]_{tit} = 0.020$ M; (×) Tit. 3, $[Ag^+]_0 = 1.0 \times 10^{-3}$ M, $[PTA]_{tit} = 0.051$ M, $[H^+]_0 = 0.05 \times 10^{-3}$ M; (●) Tit. 4 $[Ag^+]_0 = 1.0 \times 10^{-3}$ M, $[PTA]_{tit} = 0.050$ M, $[H^+]_0 = 0.9 \times 10^{-3}$ M (analytical concentrations of the species are reported in Table S3†). Symbols: experimental Q^{tot}; dashed lines: calculated Q^{tot}. Some experimental points were omitted for clarity.

$-T\Delta S_{2,Ag} < -T\Delta S_{3,Ag}$). The value of $T\Delta S_{4,Ag}$ becomes extremely negative (about twice $T\Delta S_{3,Ag}$) whereas $-\Delta H_{4,Ag} > -\Delta H_{3,Ag}$: this is compatible with a change in the coordinative structure at the metal center, from trigonal to tetrahedral without the displacement of water molecules from the solvation sphere of the metal ion.

A comparison between the stepwise thermodynamic data for the formation of $[Ag(PTA)]^+$ and $[Ag(HPTA)]^{2+}$ or $[Ag(PTA)_2]^+$ and $[Ag(HPTA)_2]^{3+}$ shows that the protonated complexes are less stable than the corresponding unprotonated ones, mainly due to the less favorable complexation enthalpy. This result can be explained by the electrostatic repulsion between the metal cation and the positively charged ligand.

The system Cu(I)–PTA was first investigated by cyclic voltammetry to check whether both Cu(I) and Cu(II) form stable complexes with PTA and, if possible, determine their redox potentials. The voltammetric analysis was performed in 1.0 M NaCl solutions, where both Cu(I) and Cu(II) form complexes of the general formula $[CuCl_m]^{1-m}$ and $[CuCl_m]^{2-m}$, respectively. Fig. 3 shows voltammetric curves recorded for Cu(I) (black line) and PTA (dotted line) separately, and for the Cu(I)–PTA mixtures at 298 K. PTA shows an irreversible oxidation peak at 0.78 V, whereas Cu(I) exhibits a reversible peak couple due to the one electron oxidation of $[CuCl_m]^{1-m}$ to $[CuCl_m]^{2-m}$. The standard potential of the Cu(II)/Cu(I) couple was estimated as the half-sum between the anodic (E_{pa}) and cathodic (E_{pc}) peak potentials: $E^\circ = (E_{pa} + E_{pc})/2 = 0.22$ V *vs.* SCE. The progressive addition of PTA resulted in a decrease of the anodic peak of $[CuCl_m]^{1-m}$ and the appearance of a new irreversible oxidation peak at $E_{pa} = 0.46$ V (Fig. 3, blue and green traces). Further

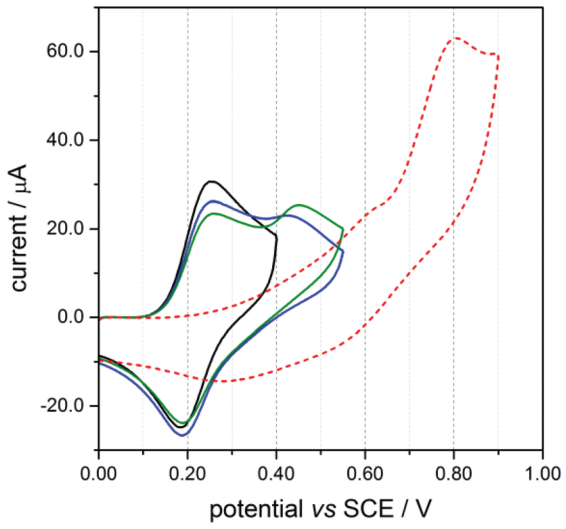

Fig. 3 Cyclic voltammetry of 4 mM PTA (dotted line) and 1 mM CuCl in 1.0 M NaCl solution in the absence (black line) and in the presence of PTA at a ligand to metal ratio of 0.1 (blue line) or 0.2 (green line); scan rate = 0.2 V s^{-1}.

addition of PTA up to a four-fold excess over Cu(I) led to a complete disappearance of the $[CuCl_m]^{1-m}$ peak and a positive shift of the new anodic peak to 0.53 V (Fig. S1†). The new anodic peaks at 0.46 and 0.53 V can be assigned to Cu(I)–PTA complexes, the first to a 1 : 1 complex and the second to $[Cu(PTA)_4]^+$. Note that both peaks are irreversible, clearly indicating that Cu(II)–PTA is not stable (see the ESI† for further details on the stability of Cu(II) in the presence of PTA). Species with 1 : 2 and 1 : 3 Cu(I)/PTA stoichiometries could not be observed because of solubility reasons. The irreversibility of the oxidation peaks precluded the possibility of determining the standard potentials, but the peak potentials provide a clear indication that PTA stabilizes Cu(I) through the formation of different complexes by the sequential addition of a metal ion.

Overall, the results indicate that: (i) the redox system of the couple Cu(I)/Cu(II) is reversible; (ii) Cu(I) is stabilized with respect to Cu(II) in 1.0 M NaCl (shift of $E°$ from +0.153 V in water[55] to +0.22 V in 1 M NaCl, respectively); (iii) Cu(I)–PTA complexes are more stable towards oxidation than the copper chloride complexes, $CuCl_m^{1-m}$; (iv) Cu(II) does not form stable complexes with PTA.

Results of the UV-vis study on the Cu(I)/PTA system show that the formation of Cu(I)–phosphine complexes significantly increases the system absorbance in the region 210–260 nm (Fig. S1 in the ESI, analytical data in Table S2†). The best fit between the calculated and experimental absorbances was obtained by assuming the formation of four consecutive complexes ($[Cu(PTA)_n]^+$, n = 1–4), whose formation constants were determined (Table 1). Fig. 4 shows the good consistency of the calculated and experimental absorbances.

Symbols in Fig. 5 show the cumulative reaction heats of some of the microcalorimetric titrations. The values of the formation constants for the first three successive $[Cu(PTA)_n]^+$ complexes (n = 1–3) obtained from the refinement of the microcalorimetric data are in very good agreement with the corresponding one determined from the spectroscopic ones (Table 1); $\log \beta_4$ (UV-Vis) is, instead, about one order of magnitude higher than $\log \beta_4$ (microcal). We selected the set of stability constant values determined by the treatment of the microcalorimetric data, since the minimization of spectroscopic data revealed a high statistical correlation between the values of $\log \beta_3$ and $\log \beta_4$.

The stepwise enthalpies of formation of the first two complexes of Cu(I) are more favourable than those of the third and fourth ones, while the corresponding entropic terms ($T\Delta S_{Cu,j}$)

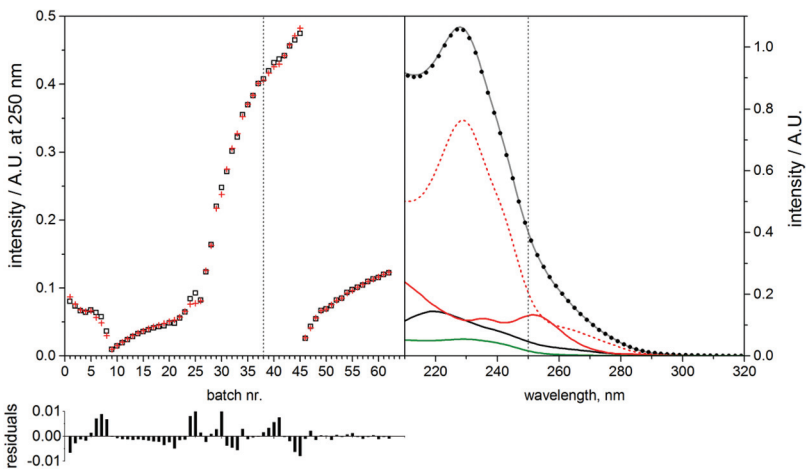

Fig. 4 Left: the fitting of spectrophotometric data: (□) calculated absorbance, (+) experimental absorbance at λ = 250 nm, collected for the spectrophotometric study (analytical details in Table S2, spectra in Figure S1, ESI†). Right: experimental (solid line) and calculated (black dots) spectra of a solution of $[Cu^+]$ = 0.05 mM, [PTA] = 0.10 mM (batch 38 in Table S2, ESI;† some of the points were skipped for clarity). Lines represent the individual spectral contribution of the four phosphine complexes: $[Cu(PTA)]^+$, solid black; $[Cu(PTA)]_2^+$, solid red; $[Cu(PTA)]_3^+$, dotted red; $[Cu(PTA)]_4^+$, solid green.

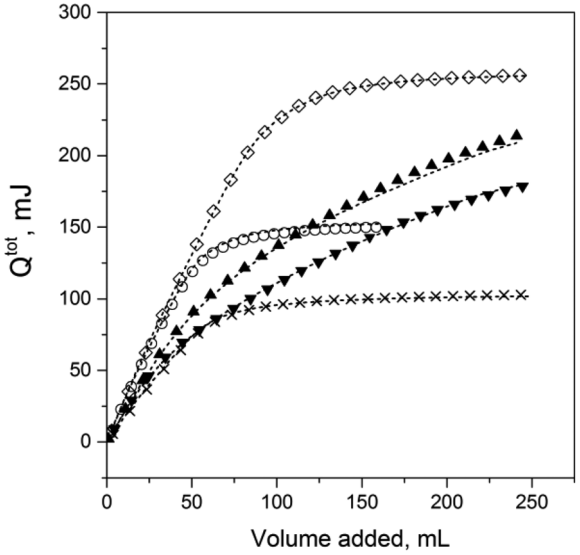

Fig. 5 Overall experimental heat (Q^{tot}) *vs.* R_c. (×) Tit. 1, $[Cu^+]_0$ = 0.20 mM, $[H^+]_0$ = 0.02 mM; (○) Tit. 2, $[Cu^+]_0$ = 0.30 mM, $[H^+]_0$ = 0.03 mM; (◊) Tit. 3, $[Cu^+]_0$ = 0.50 mM, $[H^+]_0$ = 0.05 mM; (▼) Tit. 7, $[Cu^+]_0$ = 0.20 mM, $[H^+]_0$ = 2.0 mM, (▲); Tit. 8 $[Cu^+]_0$ = 0.30 mM, $[H^+]_0$ = 1.8 mM, (analytical data also in the ESI, Table S3†). Dots: experimental Q^{tot}; dashed lines: Q^{tot} calculated with ΔH_j and log β_j in Table 1. For the sake of clarity, some experimental points are omitted.

follow a swinging trend. The enthalpy of formation of the third complex is about 19 kJ mol^{-1} less favourable than that of the second, while $T\Delta S_{Cu,3}$ is 18 kJ mol^{-1} more favourable (less negative) than $T\Delta S_{Cu,2}$. Apparently, the reaction for the formation of the third complex is the one that entails major changes in the system state. Although the enthalpy contributions are similar in the third and fourth steps ($\Delta H_{Cu,4}$ = −40 kJ mol^{-1} and $\Delta H_{Cu,3}$ = −38 kJ mol^{-1}), $T\Delta S_{Cu,4}$ is about 13 kJ mol^{-1} more unfavourable than $T\Delta S_{Cu,3}$. This makes K_4 about two orders of magnitude smaller than K_3.

These data are difficult to rationalize, but it should be considered that thermodynamic data in Table 1 refer to a 1.0 M chloride medium (*i.e.* to formation equilibria (1) and (2) where the phosphine complexes result from a total or partial substitution of chloride ions in the coordination sphere of the copper ion).

Therefore, the interpretation of the trend in thermodynamic data must take into account the role of the chloride ion. For this reason, a detailed DFT study on the stoichiometry and the relative stabilities of the complexes in equilibria (1) and (2) has been carried out.

DFT calculations

Among the possible starting structures considered for geometry optimizations within the DFT calculations (Tables S4 and S5†), several complexes dissociate releasing one or more ligands, leading to a limited number of stable final products. The structures of the stable complexes are shown in Fig. 6 and relevant bond lengths are reported in Table 2. Differently from our previous approach, where the stepwise formation para-

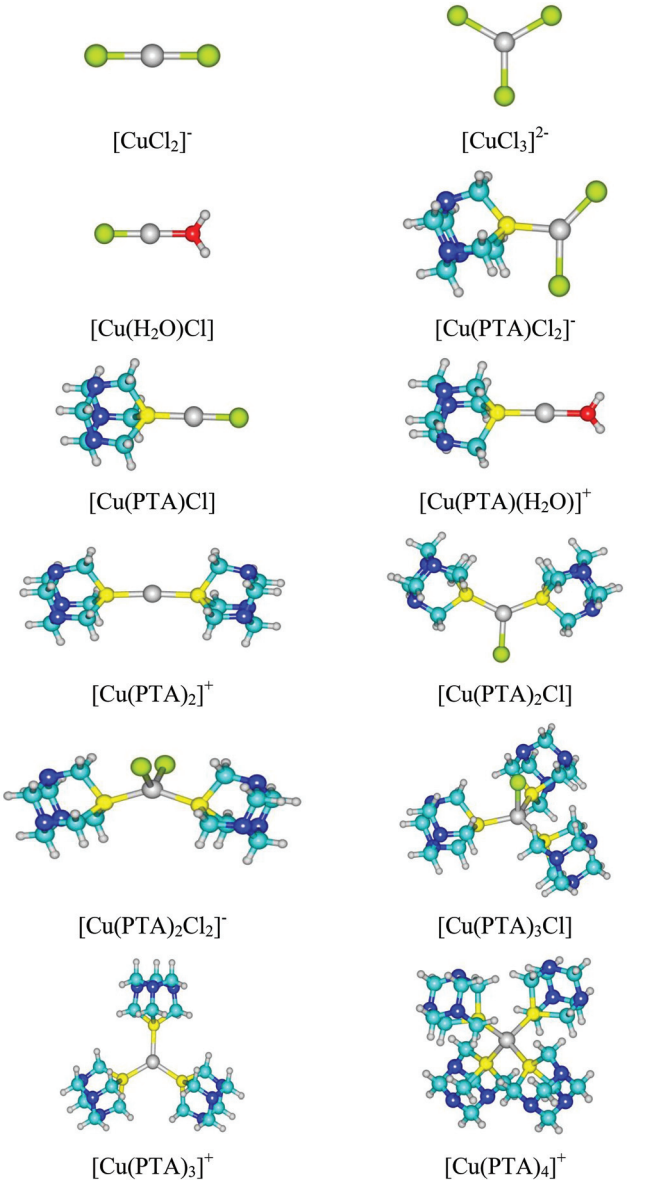

Fig. 6 Optimized structures of the $[Cu(PTA)_n(Cl)_m(H_2O)_l]^{1-m}$ complexes.

Table 2 Cu–Cl, Cu–O and Cu–P calculated bond lengths (Å). Available experimental values in parentheses

Complex	r_{Cu-Cl}	r_{Cu-P}	r_{Cu-O}
$[CuCl_2]^-$	2.156(2.13)[a]	—	—
$[CuCl_3]^{2-}$	2.384(2.235)[b]	—	—
$[Cu(H_2O)Cl]$	2.085	—	1.966
$[Cu(PTA)Cl]$	2.115	2.177	—
$[Cu(H_2O)(PTA)]^+$	—	2.184(2.149)[c]	1.967
$[Cu(PTA)Cl_2]^-$	2.335/2.236	2.279	—
$[Cu(PTA)_2]^+$	—	2.244	—
$[Cu(PTA)_2Cl]$	2.237	2.267	—
$[Cu(PTA)_2Cl_2]^-$	2.436	2.268(2.228)[d]	—
$[Cu(PTA)_3Cl]$	2.411	2.307(2.226)[e]	—
$[Cu(PTA)_3]^+$	—	2.311	—
$[Cu(PTA)_4]^+$	—	2.364 (2.298)	—

[a] Ref. 60. [b] Ref. 61. [c] Ref. 62. [d] Ref. 63. [e] $[Cu(PTA)_3I]$ ref. 64.

meters for each complex were reported,[56–58] here we focus on the relative stability of each $[Cu(PTA)_nCl_m(H_2O)_l]^{1-m}$ (n = 0–4; m = 0–2; $n + m$ = 1–4) complex. The free energies for the reactions reported in Table 3 were calculated to compare the relative stability of pairs of Cu^+–Cl^-–PTA species and predict the most likely stoichiometry and structure of the species existing in solution.

The optimization of the $[CuCl_m(H_2O)_l]^{1-m}$ (m, $l \leq 4$) structures produced only three stable final products $[CuCl_2]^-$, $[CuCl_3]^{2-}$, $[CuCl(H_2O)]$ (Fig. 6), due to the dissociation of either two chlorides or water molecules from the other complexes considered (Table 3). In all structures the calculated Cu–Cl bond lengths are slightly overestimated with respect to the available experimental values (Table 2), as is often observed for geometry optimizations with CGA DFT methods.[31,59] The calculated Cu–Cl distance for the linear $[CuCl_2]^-$ complex is 2.156 Å, in good agreement with the experimental value of 2.13 Å.[60] Notably, the Cu–Cl distance in the planar trigonal $[CuCl_3]^{2-}$ complex calculated in this work (2.384 Å) is significantly larger than that obtained by the fitting of XANES spectra (2.235 Å).[61] It is interesting to note that, according to the results of the present study, the fitting of XANES spectra by Brugger *et al.*[61] is not compatible with the presence of the complex $[CuCl_4]^{3-}$ in solution even at high chloride concentrations.

Three stable 1 : 1 Cu : PTA complexes have been obtained: in two of them ([Cu(PTA)Cl] and $[Cu(PTA)(H_2O)]^+$) the copper ion is linearly coordinated, while the third complex ($[Cu(PTA)Cl_2]^-$) has a trigonal distorted geometry (Fig. 6). The calculated Cu–P bond distances in these complexes (2.177–2.189 Å) are in good agreement with the value found in the crystal structure of the only available 1 : 1 Cu/PTA complex (2.149 Å).[62] Attempts to optimize $[Cu(PTA)Cl_m(H_2O)_l]^{1-m}$ (m = 0–2, l = 1–2) complexes always resulted in the dissociation of water molecule(s) (Table S4†).

The thermodynamic parameters in Table 3 show that [Cu(PTA)Cl] is much more stable than $[Cu(PTA)Cl_2]^-$ and $[Cu(PTA)(H_2O)]^+$ since the Gibbs free energies of reactions (a) and (b) in water are markedly positive. It is remarkable that the higher stability of [Cu(PTA)Cl] than $[Cu(PTA)Cl_2]^-$ in water is largely due to the introduction of solvation, since $[Cu(PTA)Cl_2]^-$ is the more stable complex in the gas phase. In conclusion, DFT calculations are compatible with the fact that in chloride solution the actual 1 : 1 Cu : PTA complex should be [Cu(PTA)Cl].

Calculations on structures with a 1 : 2 Cu : PTA stoichiometry demonstrated that three stable complexes $[Cu(PTA)_2Cl_m]^{1-m}$ can be formed. In this case, the copper ion can assume a linear, trigonal or distorted tetrahedral coordination geometry when m = 0, 1, 2 respectively (Fig. 6). Also in this case our calculations perform reasonably well in predicting the geometries of the complexes (Table 2).[63] Attempts to optimize $[Cu(PTA)_2Cl_m(H_2O)_l]^{1-m}$ (m = 0–2, l = 1–2) resulted in the dissociation of the water molecule(s) (Table S4†).

The free energies of the reactions (c) and (d) in Table 3 show that $[Cu(PTA)_2Cl]$ is the most stable complex among those considered. However, the relatively small ΔG° in reaction (d) suggests that a considerable fraction of $[Cu(PTA)_2]^+$ should be present in equilibrium with $[Cu(PTA)_2Cl]$.

The optimization of $[Cu(PTA)_3Cl_m]^{1-m}$ (m = 0, 1) structures shows that both complexes, where Cu(I) has respectively, a trigonal planar or pyramidal geometry, are thermodynamically stable in water. In this case, the Cu–P bond lengths (Table 2) are in good agreement with those found in the isostructural compound $[Cu(PTA)_3I]$.[64] According to the ΔG° of the reaction (e), the most stable of these species in water is $[Cu(PTA)_3]^+$, while the opposite is found in the gas phase.

Finally, the optimization of $[Cu(PTA)_4]^+$ resulted in a distorted tetrahedral structure with the Cu–P bond slightly longer than that experimentally determined.[64] The positive ΔG° for the reaction (f) in water suggests that $[Cu(PTA)_4]^+$ is less stable than $[Cu(PTA)_3]^+$, hence its formation in solution should occur only at very high PTA/Cu molar ratios.

On the basis of the results of DFT calculations it was possible to sort out the stoichiometry of the different $[CuCl_m(PTA)_n]^{1-m}$ species estimated to be more stable in aqueous solution. The stepwise formation reactions (4)–(8) can be therefore proposed, where the hidden role of chloride is revealed:

$$[CuCl_2]^- + PTA = Cu(PTA)Cl + Cl^- \quad (4)$$

$$[CuCl_3]^{2-} + PTA = Cu(PTA)Cl + 2Cl^- \quad (5)$$

$$Cu(PTA)Cl + PTA = Cu(PTA)_2Cl \quad (6)$$

$$Cu(PTA)_2Cl + PTA = [Cu(PTA)_3]^+ + Cl^- \quad (7)$$

$$[Cu(PTA)_3]^+ + PTA = [Cu(PTA)_4]^+ \quad (8)$$

In agreement with the DFT calculations the most likely stoichiometry of the first Cu/PTA complex is [Cu(PTA)Cl](aq) bearing a linear structure (Fig. 6). The formation of this species involves the displacement of one (eqn (4)) and two (eqn (5)) chloride ions from $[CuCl_2]^-$ and $[CuCl_3]^{2-}$, respectively. This could explain the higher formation entropy of the first complex, relative to the second, also compatible with the removal of one or two negative ions from the coordination sphere of the metal cation.

The positive free energy changes of reactions (c) and (d) in Table 3 and the structures in Fig. 6 indicate that the complex with a Cu/PTA = 1 : 2 stoichiometry is [Cu(PTA)Cl](aq), formed without the removal of chloride from the acceptor (eqn (6)) and involving a structure change from linear to planar

Table 3 Thermodynamic quantities (kJ mol^{-1}) of reactions of the Cu^+–Cl^-–PTA system calculated in vacuum and in PCM water

		ΔG°_{gas}	ΔG°_{water}
(a)	$[Cu(PTA)Cl] + Cl^- \rightarrow [Cu(PTA)Cl_2]^-$	−82.0	19.7
(b)	$[Cu(PTA)Cl] + H_2O \rightarrow [Cu(PTA)(H_2O)]^+ + Cl^-$	484.5	54.1
(c)	$[Cu(PTA)_2Cl] + Cl^- \rightarrow [Cu(PTA)_2Cl_2]^-$	−79.9	32.7
(d)	$[Cu(PTA)_2Cl] \rightarrow [Cu(PTA)_2]^+ + Cl^-$	418.4	18.4
(e)	$[Cu(PTA)_3]^+ + Cl^- \rightarrow [Cu(PTA)_3Cl]$	−382.4	13.8
(f)	$[Cu(PTA)_3]^+ + PTA \rightarrow [Cu(PTA)_4]^+$	5.9	28.9

Table 4 The overall and stepwise conditional formation constants of Cu(I)–PTA complexes (obs) in 1.0 M NaCl and the corresponding estimated values (est) in a non-complexing ionic medium compared with the values for Ag(I) complexes in 0.1 M $NaNO_3$. T = 298 K. L = PTA. More details available in the ESI

	M = Cu^+		M = Ag^+
Overall	$\log \beta_{j,obs}$	$\log \beta_{j,est}$ (σ)	$\log \beta_{j,obs}$
M + L = ML	6.3	8.9(3)	8.19
M + 2L = ML_2	12.1	15.9(12)	13.67
M + 3L = ML_3	17.7	22.7(1)	17.67
M + 4L = ML_4	21.4	26.4(1)	20.35
Stepwise	$\log K_{j,obs}$	$\log K_{j,est}$	$\log K_{j,obs}$
M + L = ML	6.3	8.9	8.19
ML + L = ML_2	5.8	8.5	5.48
ML_2 + L = ML_3	5.6	5.3	4.00
ML_3 + L = ML_4	3.7	3.7	2.68

trigonal. This supports the more favourable stepwise enthalpy and the trend in entropy of formation.

$[Cu(PTA)_3]^+$ forms according to eqn (7). The reaction occurs without structural changes but with the removal of one chloride ion from the acceptor. The enthalpy decrease passing from the second to the third complex may be a consequence of the energy demand due to the removal of one chloride from the coordination sphere of the metal. Conversely, the remarkable increase of the corresponding reaction entropy ($T\Delta S_{Cu,2} = -24$, $T\Delta S_{Cu,3} = -6$ kJ mol^{-1}) may suggest both a dwindling solvation of the complex and a corresponding entropy gain that occurs when a PTA molecule substitutes a chloride ion into the coordination sphere of the metal, without coordination changes.

Eqn (8) indicates that the formation of $[Cu(PTA)_4]^+$ occurs with a transition of the coordinative geometry of the metal core, from a trigonal arrangement in $[Cu(PTA)_3]^+$ to the tetrahedral one in $[Cu(PTA)_4]^+$. The large decrease in entropy for the formation of $[Cu(PTA)_4]^+$ can be connected with the severe losses in the ligand conformational entropies.

Based on the combined indications from DFT calculations and thermodynamic data, we estimated the affinity of PTA for Cu(I) in the absence of chloride. The values of the formation constants of the successive species Cu(I)–PTA, accordingly corrected, are listed in Table 4. The values of the $\log \beta_{Cu,n}$ of $[Cu(PTA)_3]^+$ and $[Cu(PTA)_4$ were increased by 5.0 log units, an average value accounting for the quantitative removal of chloride from Cu(I), initially existing as CuCl(aq), $CuCl_2^-$ and $CuCl_3^{2-}$ ($\log \beta_{CuCl_n} \approx 0.03 \times 2.68 + 0.660 \times 5.07 + 0.337 \times 4.78 \approx 5.0$).§ The values of the $\log \beta_{Cu,n}$ of $[Cu(PTA)]^+$ and $[Cu(PTA)_2]^+$ were increased by ~2.6 and ~3.8 log units, to reflect the formation of the mixed Cu(I)/PTA/Cl^- complexes [Cu(PTA)Cl](aq) and $[Cu(PTA)_2Cl](aq)$.

Cu(I) and Ag(I) complexes with PTA in a non-complexing medium

In Table 4 the estimated values of the overall and stepwise conditional formation constants of Cu(I)–PTA complexes in a non-complexing ionic medium are compared with the corresponding values for Ag(I) complexes in 0.1 M $NaNO_3$. We consider the comparison reasonable, even if the stability data of Ag(I) and Cu(I) refer to different ionic medium concentrations, because the difference in $\log \beta$s in the two ionic media is within the mean error we attribute to the estimated values of the stability constants of Cu(I) complexes (±0.3–1.0 log units).

As expected according to the HSAB theory,[52] the formation of Cu(I)–PTA complexes is favored with respect to that of Ag(I) in all the consecutive complexation steps. However, the ratios between the consecutive formation constants are very different for the two metal ions (K_1/K_2, K_2/K_3, K_3/K_4 = 2.5, 1549, 400 and 513, 30, 21 for Cu(I) and Ag(I), respectively). Apparently, $[Cu(PTA)_2]^+$ and $[Ag(PTA)]^+$ are the complexes with the largest range of existence under these conditions. Speciation plots in Fig. 7 reflect these findings. The figure shows the relative abundance of Cu(I) and Ag(I) complexes at different ligand to metal molar ratios, in aqueous solutions at pH 7.3, close to that of biological systems. The two distributions refer to a total concentration of Cu^+ or Ag^+ of 10^{-5} M, close to those used by Tisato *et al.*[65] in the mass spectrometry study on $[M(PTA)_4][PF_6]$ solutions. The distribution of the species when the solid compounds are dissolved in solution (*i.e.* when $[PTA]/[M^+] = 4$), indicates that both the copper and silver compounds are partially dissociated, in agreement with the

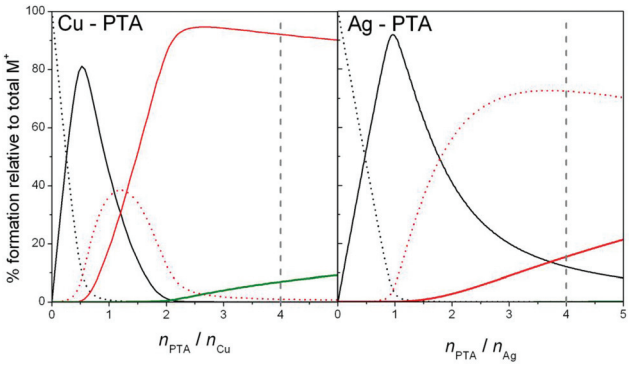

Fig. 7 Percentage distribution of the Cu(I)–PTA (left) and Ag(I)–PTA species (right) as a function of n_{PTA}/n_M (M = Cu, Ag), in solutions with a total concentration of $[Cu^+]$, $[Ag^+] = 10^{-5}$ M; pH_M = 7.3; I = 1.0 M NaCl (Cu(I)–PTA) or 0.1 M $NaNO_3$ (Ag(I)–PTA). Formation constants of the species listed in Table 4 ($\log \beta_{j,est}$ for Cu(I)–PTA complexes and $\log \beta_{j,obs}$ for Ag(I)–PTA ones). In the diagrams: dotted black: M^+; solid black: $M(PTA)^+$; dotted red: $M(PTA)_2^+$; solid red: $M(PTA)_3^+$; solid green: $M(PTA)_4^+$; dashed grey vertical line: in-solution distribution of the different species predicted by the p.w., when the solid compounds $M(PTA)_4[X]$ (M^+ = Cu^+, Ag^+; X^- = BF_4^-, PF_6^-) are dissolved in solution, with a concentration 10^{-5} M.

§ Note that in 1968 Raymond and Bjerrum[68] suggested a different approach to evaluate the correction factor on $\log \beta_3$ and $\log \beta_4$ of a couple of Cu(I) phosphine complexes, based on the relative concentration of the Cu(I) aqua ion in 1 M Cl^- solution.[68] The value of the correction factor obtained with Bjerrum's approach is near to the one we have calculated (5.2 *vs.* 5.0) but the applicability of the approach appears to be more limited.

evidence from mass spectrometry.[65] However, according to our results, $[Cu(PTA)_3]^+$ is the most abundant species in solution. The previous MS characterization[12] conversely indicated $[Cu(PTA)_2]^+$ as the most abundant species. It is difficult to rationalize the disagreement in the speciation of Cu(I) predicted by the two techniques. This could be attributed to an enhanced signal of the $[Cu(PTA)_2]^+$ species in the ESI-MS experiments, which has been reported to depend on the instrumental parameters chosen, such as the potential applied to generate the electrospray.[66,67] The same difference could be attributed to an incorrect estimation of $\log \beta_{j,est}$ (Table 4) for the successive Cu–PTA species, used to trace the distribution diagrams in Fig. 7 (left). It is worth noticing that a similar distribution of the different Cu–PTA species is obtained using the values experimentally determined ($\log \beta_{j,obs}$, Table 4). Also in the latter case, $[Cu(PTA)_3]^+$ is predicted to be the most abundant species at *ca.* 10^{-5} M. On the basis of the present findings and the previous indications from the MS study, we therefore suggest $[Cu(PTA)_2]^+$, $[Cu(PTA)_3]^+$ and $[Ag(PTA)_2]^+$ as the species mainly involved in the cytotoxic activity of the tetracoordinated compounds $M(PTA)_4[X]$ (M = Cu, Ag; X = BF_4, PF_6).

Conclusions

The formation equilibria of a series of Cu(I) and Ag(I) complexes with PTA in aqueous solution were studied by means of microcalorimetric, potentiometric and spectrophotometric techniques to provide accurate values of the thermodynamic functions concerning the formation of the $[M(PTA)_n]^+$ complexes (n = 1–4) with M = Cu(I), Ag(I). A new experimental approach which combines anoxic conditions and 1.0 M NaCl solutions is proposed to study the Cu(I)–PTA complex formation. The background electrolyte is also a complexing medium for Cu(I) stabilizing this monovalent cation.

Thermodynamic data in solution have been combined with the results of DFT calculations to obtain a better insight about the nature and stoichiometry of the complex formation. Theoretical data show that only a limited number of the $[Cu(PTA)_nCl_m(H_2O)_l]^{1-m}$ complexes (n = 0–4; m = 0–4; l = 1, 2) can be obtained, since in several cases the dissociation of one ligand occurs during the geometry optimization. The most stable 1 : 1 Cu(I)/PTA complex retains one chloride in the first coordination sphere in the 1 : 1 species. A different result is found for the 1 : 2 Cu/PTA complex where $[Cu(PTA)_2Cl]$ and $[Cu(PTA)_2]^+$ are predicted to have a similar stability. In the 1 : 3 Cu–PTA species, the most stable complex is $[Cu(PTA)_3]^+$, suggesting that only at this stage Cl^- is completely released from copper.

On the basis of theoretical and thermodynamic data, new values of the "true" stability constants for the Cu(I)–PTA complexes have been estimated. This allows a direct comparison with the analogous Ag(I) systems studied in a non-complexing medium. The speciation obtained shows that both the silver and the copper complexes are tetracoordinated species in the solid state and in solution at relatively high concentrations ($>10^{-2}$ M). However, they are dissociated to lower stoichiometry species when diluted in the micromolar range typical of *in vitro* biological testing.

The approach employed in this work is a general-purpose method to account for the hidden role of chloride ions and thus to evaluate the "true" affinity of Cu(I) for any ligand in a non-complexing medium.

Acknowledgements

The Italian consortium CINECA is acknowledged by A. M. for computing time (project "IscrC_M2015-3").

References

1 D. M. Medeiros and D. Jennings, *J. Bioenerg. Biomembr.*, 2002, **34**, 389.
2 I. Iakovidis, I. Delimaris and S. M. Piperakis, *Mol. Biol. Int.*, 2011, 594529.
3 L. Yang, Z. Huang and F. Li, *J. Pept. Sci.*, 2012, **18**(7), 449–455.
4 I. Voskoboinik and J. Camakaris, *J. Bioenerg. Biomembr.*, 2002, **34**, 363–371.
5 S. Lutsenko, R. G. Efremov, R. Tsivkovskii and J. M. Walker, *J. Bioenerg. Biomembr.*, 2002, **34**, 351–362.
6 J. T. Rubino, P. Riggs-Gelasco and K. J. Franz, *J. Biol. Inorg. Chem.*, 2010, **15**, 1033–1049.
7 J. T. Rubino, M. P. Chenkin, M. Keller, P. Riggs-Gelasco and K. J. Franz, *Metallomics*, 2011, **3**, 61–73.
8 P. A. Cobine, L. D. Ojeda, K. M. Rigby and D. R. Winge, *J. Biol. Chem.*, 2004, **279**, 14447–14455.
9 P. A. Cobine, F. Pierrel and D. R. Winge, *Biochim. Biophys. Acta, Mol. Cell Res.*, 2006, **1763**, 759–772.
10 E. Georgatsou, L. A. Mavrogiannis, G. S. Fragiadakis and D. Alexandraki, *J. Biol. Chem.*, 1997, **272**, 13786–13792.
11 C. Santini, M. Pellei, G. Papini, B. Morresi, R. Galassi, S. Ricci, F. Tisato, M. Porchia, M. P. Rigobello, V. Gandin and C. Marzano, *J. Inorg. Biochem.*, 2011, **105**, 232–240.
12 F. Tisato, F. Refosco, M. Porchia, M. Tegoni, V. Gandin, C. Marzano, M. Pellei, G. Papini, L. Lucato, R. Seraglia and P. Traldi, *Rapid Commun. Mass Spectrom.*, 2010, **24**, 1610–1616.
13 C. Marzano, V. Gandin, M. Pellei, D. Colavito, G. Papini, G. G. Lobbia, E. Del Giudice, M. Porchia, F. Tisato and C. Santini, *J. Med. Chem.*, 2008, **51**, 798–808.
14 C. Santini, M. Pellei, V. Gandin, M. Porchia, F. Tisato and C. Marzano, *Chem. Rev.*, 2014, **114**, 815–862.
15 F. Tisato, C. Marzano, V. Peruzzo, M. Tegoni, M. Giorgetti, M. Damjanovic, A. Trapananti, A. Bagno, C. Santini, M. Pellei, M. Porchia and V. Gandin, *J. Inorg. Biochem.*, 2016, **165**, 80–91.
16 S. W. Jaros, M. F. C. Guedes da Silva, M. Florek, P. Smoleński, A. J. L. Pombeiro and A. M. Kirillov, *Inorg. Chem.*, 2016, **55**, 5886–5894.

17 S. W. Jaros, M. F. C. Guedes da Silva, M. Florek, M. C. Oliveira, P. Smoleński, A. J. L. Pombeiro and A. M. Kirillov, *Cryst. Growth Des.*, 2014, **14**, 5408–5417.
18 P. Smolenski, S. W. Jaros, C. Pettinari, G. Lupidi, L. Quassinti, M. Bramucci, L. A. Vitali, D. Petrelli, A. Kochel and A. M. Kirillov, *Dalton Trans.*, 2013, **42**, 6572–6581.
19 A. Lis, M. F. C. Guedes da Silva, A. M. Kirillov, P. Smoleński and A. J. L. Pombeiro, *Cryst. Growth Des.*, 2010, **10**, 5244–5253.
20 A. M. Kirillov, P. Smoleński, M. Haukka, M. F. C. Guedes da Silva and A. J. L. Pombeiro, *Organometallics*, 2009, **28**, 1683–1687.
21 A. M. Kirillov, P. Smolenski, M. F. C. Guedes da Silva, M. N. Kopylovich and A. J. L. Pombeiro, *Acta Crystallogr., Sect. E: Struct. Rep. Online*, 2008, **64**, m603–m604.
22 M. Fátima, C. Guedes, A. M. Kirillov, P. Smolen and A. J. L. Pombeiro, *Eur. J. Inorg. Chem.*, 2007, 2686–2692.
23 V. K. Sharma and F. J. Millero, *J. Solution Chem.*, 1990, **19**, 375–390.
24 P. Di Bernardo, A. Melchior, R. Portanova, M. Tolazzi and P. L. L. Zanonato, *Coord. Chem. Rev.*, 2008, **252**, 1270–1285.
25 S. Del Piero, R. Fedele, A. Melchior, R. Portanova, M. Tolazzi and E. Zangrando, *Inorg. Chem.*, 2007, **46**, 1406–1406.
26 A. Melchior, E. Peralta, M. Valiente, C. Tavagnacco, F. Endrizzi and M. Tolazzi, *Dalton Trans.*, 2013, **42**, 6074–6082.
27 A. Melchior, E. Peralta, M. Valiente and M. Tolazzi, *Polyhedron*, 2014, **75**, 88–94.
28 B. Sarkar, *Chem. Rev.*, 1999, **99**, 2535.
29 A. C. Mendonca, A. F. Martins, A. Melchior, S. M. Marques, S. Chaves, S. Villette, S. Petoud, P. L. Zanonato, M. Tolazzi, C. S. Bonnet, E. Toth, P. Di Bernardo, C. F. G. C. Geraldes and M. A. Santos, *Dalton Trans.*, 2013, **42**, 6046–6057.
30 F. Endrizzi, A. Melchior, M. Tolazzi and L. Rao, *Dalton Trans.*, 2015, **44**, 13835–13844.
31 A. Melchior, E. Sánchez Marcos, R. R. Pappalardo and J. M. Martínez, *Theor. Chem. Acc.*, 2011, **128**, 627–638.
32 A. Melchior, J. M. Martínez, R. R. Pappalardo and E. Sánchez Marcos, *J. Chem. Theor. Comput.*, 2013, **9**, 4562–4573.
33 A. Melchior, M. Tolazzi, J. M. Martínez, R. R. Pappalardo and E. Sánchez Marcos, *J. Chem. Theor. Comput.*, 2015, **11**, 1735–1744.
34 M. M. Dell'Anna, V. Censi, B. Carrozzini, R. Caliandro, N. Denora, M. Franco, D. Veclani, A. Melchior, M. Tolazzi and P. Mastrorilli, *J. Inorg. Biochem.*, 2016, **163**, 346–361.
35 D. J. Daigle, T. J. Decuir, J. B. Robertson and D. J. Darensbourg, *1,3,5-Triaza-7-phosphatricyclo[3.3.1.13,7] decane and derivatives*, John Wiley & Sons, Hoboken, NJ, USA, 1998, vol. 32.
36 W. L. F. Armarego and C. L. L. Chai, *Butterworth-Heinemann*, Oxford, 2009, pp. 445–576.
37 G. H. Jeffrey, J. Bassett, J. Mendham and R. C. Denney, *Vogel's textbook of quantitative chemical analysis*, John Wiley & Sons, 5th edn, 1990, vol. 14.
38 J. Brugger, B. Etschmann, W. Liu, D. Testemale, J. L. Hazemann, H. Emerich, W. van Beek and O. Proux, *Geochim. Cosmochim. Acta*, 2007, **71**, 4920–4941.
39 L. Ciavatta and M. Iuliano, *Ann. Chim.*, 1998, **88**, 71–89.
40 Z. Xiao, C. H. Gammons and A. E. Williams-Jones, *Geochim. Cosmochim. Acta*, 1998, **62**, 2949–2964.
41 P. Gans, A. Sabatini and A. Vacca, *Talanta*, 1996, **43**, 1739–1753.
42 L. Toso, G. Crisponi, V. M. Nurchi, M. Crespo-Alonso, J. I. Lachowicz, M. A. Santos, S. M. Marques, J. Niclós-Gutiérrez, J. M. González-Pérez, A. Domínguez-Martín, D. Choquesillo-Lazarte and Z. Szewczuk, *J. Inorg. Biochem.*, 2013, **127**, 220–231.
43 V. M. Nurchi, G. Crisponi, M. Arca, M. Crespo-Alonso, J. I. Lachowicz, D. Mansoori, L. Toso, G. Pichiri, M. Amelia Santos, S. M. Marques, J. Niclós-Gutiérrez, J. M. González-Pérez, A. Domínguez-Martín, D. Choquesillo-Lazarte, Z. Szewczuk, M. Antonietta Zoroddu and M. Peana, *J. Inorg. Biochem.*, 2014, **141**, 132–143.
44 R. Arnek, *Ark. Kemi*, 1970, **32**, 81–88.
45 P. Di Bernardo, P. Zanonato, L. Rao, A. Bismondo and F. Endrizzi, *Dalton Trans.*, 2011, **40**, 9101–9105.
46 C. T. Lee, W. T. Yang and R. G. Parr, *Phys. Rev. B*, 1988, **37**, 785–789.
47 A. D. Becke, *J. Chem. Phys.*, 1993, **98**, 1372–1377.
48 M. Dolg, U. Wedig, H. Stoll and H. Preuss, *J. Chem. Phys.*, 1987, **86**, 866–872.
49 J. Tomasi, B. Mennucci and R. Cammi, *Chem. Rev.*, 2005, **105**, 2999–3094.
50 S. Vukovic, B. P. Hay and V. S. Bryantsev, *Inorg. Chem.*, 2015, **54**, 3995–4001.
51 M. J. Frisch, G. W. Trucks, H. B. Schlegel, G. E. Scuseria, M. A. Robb, J. R. Cheeseman, G. Scalmani, V. Barone, B. Mennucci, G. A. Petersson, H. Nakatsuji, M. Caricato, X. Li, H. P. Hratchian, A. F. Izmaylov, J. Bloino, G. Zheng, J. L. Sonnenberg, M. Hada, M. Ehara, K. Toyota, R. Fukuda, J. Hasegawa, M. Ishida, T. Nakajima, Y. Honda, O. Kitao, H. Nakai, T. Vreven, J. A. Montgomery Jr., J. E. Peralta, F. Ogliaro, M. Bearpark, J. J. Heyd, E. Brothers, K. N. Kudin, V. N. Staroverov, R. Kobayashi, J. Normand, K. Raghavachari, A. Rendell, J. C. Burant, S. S. Iyengar, J. Tomasi, M. Cossi, N. Rega, J. M. Millam, M. Klene, J. E. Knox, J. B. Cross, V. Bakken, C. Adamo, J. Jaramillo, R. Gomperts, R. E. Stratmann, O. Yazyev, A. J. Austin, R. Cammi, C. Pomelli, J. W. Ochterski, R. L. Martin, K. Morokuma, V. G. Zakrzewski, G. A. Voth, P. Salvador, J. J. Dannenberg, S. Dapprich, A. D. Daniels, Ö. Farkas, J. B. Foresman, J. V. Ortiz, J. Cioslowski and D. J. Fox, *Gaussian 09 Rev. D.01*, Gaussian Inc., Wallingford CT, 2009.
52 R. G. Pearson, *J. Chem. Educ.*, 1968, **45**, 581–587.
53 I. Persson and K. B. Nilsson, *Inorg. Chem.*, 2006, **45**, 7428–7434.
54 S. Ahrland, B. Tagesson and D. Tuhtar, *Acta Chem., Scand. Ser. A*, 1977, **31**, 625.
55 D. R. Lide, *CRC Handbook of Chemistry and Physics*, CRC Press, Taylor & Francis Group, 87th edn, 2006.
56 P. Di Bernardo, P. L. Zanonato, F. Benetollo, A. Melchior, M. Tolazzi and L. Rao, *Inorg. Chem.*, 2012, **51**, 9045–9055.

57 S. Del Piero, A. Melchior, P. Polese, R. Portanova and M. Tolazzi, *Eur. J. Inorg. Chem.*, 2006, 304–314.
58 S. Del Piero, P. Di Bernardo, R. Fedele, A. Melchior, P. Polese and M. Tolazzi, *Eur. J. Inorg. Chem.*, 2006, 3738–3745.
59 Y. Minenkov, A. Singstad, G. Occhipinti and V. R. Jensen, *Dalton Trans.*, 2012, **41**, 5526–5541.
60 J. L. Fulton, M. M. Hoffmann and J. G. Darab, *Chem. Phys. Lett.*, 2000, **330**, 300–308.
61 J. Brugger, B. Etschmann, W. Liu, D. Testemale, J. L. Hazemann, H. Emerich, W. van Beek and O. Proux, *Geochim. Cosmochim. Acta*, 2007, **71**, 4920–4941.
62 R. Wanke, P. Smoleński, M. F. C. G. da Silva, L. M. D. R. S. Martins and A. J. L. Pombeiro, *Inorg. Chem.*, 2008, **47**, 10158–10168.
63 A. M. Kirillov, M. Filipowicz, M. F. C. Guedes da Silva, J. Kłak, P. Smoleński and A. J. L. Pombeiro, *Organometallics*, 2012, **31**, 7921–7925.
64 Ł. Jaremko, A. M. Kirillov, P. Smoleński and A. J. L. Pombeiro, *Cryst. Growth Des.*, 2009, **9**, 3006–3010.
65 F. Tisato, L. Crociani, M. Porchia, P. Di Bernardo, F. Endrizzi, C. Santini and R. Seraglia, *Rapid Commun. Mass Spectrom.*, 2013, **27**, 2019–2027.
66 M. S. Espinosa, L. Folguera, J. F. Magallanes and P. A. Babay, *Chemom. Intell. Lab. Syst.*, 2015, **146**, 120–127.
67 M. S. Espinosa, R. Servant and P. A. Babay, *Microchem. J.*, 2016, **129**, 151–157.
68 G. Raymond and J. Bjerrum, *Acta Chem. Scand.*, 1968, **22**, 497–502.